Pressure-Dependent Structure Changes in Barnase on Ligand Binding Reveal Intermediate Rate Fluctuations

David J. Wilton,[†] Ryo Kitahara,[‡§] Kazuyuki Akasaka,[‡¶] Maya J. Pandya,[†] and Mike P. Williamson[†*]
[†]Department of Molecular Biology and Biotechnology, University of Sheffield, Sheffield, United Kingdom; [‡]RIKEN SPring-8 Center, Hyogo, Japan; [§]College of Pharmaceutical Sciences, Ritsumeikan University, Kusatsu, Japan; and [¶]Department of Biotechnological Science, School of Biology-Oriented Science and Technology, Kinki University, Kinokawa, Japan

ABSTRACT In this work we measured ^{1}H NMR chemical shifts for the ribonuclease barnase at pressures from 3 MPa to 200 MPa, both free and bound to d(CGAC). Shift changes with pressure were used as restraints to determine the change in structure with pressure. Free barnase is compressed by ~0.7%. The largest changes are on the ligand-binding face close to Lys-27, which is the recognition site for the cleaved phosphate bond. This part of the protein also contains the buried water molecules. In the presence of d(CGAC), the compressibility is reduced by ~70% and the region of structural change is altered: the ligand-binding face is now almost incompressible, whereas changes occur at the opposite face. Because compressibility is proportional to mean square volume fluctuation, we conclude that in free barnase, volume fluctuation is largest close to the active site, but when the inhibitor is bound, the fluctuations become much smaller and are located mainly on the opposite face. The timescale of the fluctuations is nanoseconds to microseconds, consistent with the degree of ordering required for the fluctuations, which are intermediate between rapid uncorrelated side-chain dynamics and slow conformational transitions. The high-pressure technique is therefore useful for characterizing motions on this relatively inaccessible timescale.

INTRODUCTION

The function of proteins depends not only on their three-dimensional structure, but also on their dynamics (1). Site-specific information on dynamics has come mainly from NMR, which provides information via ^{15}N relaxation measurements on rapid (picosecond/nanosecond) motions of the backbone, and via ^{13}C relaxation on side chains. More recently, NMR relaxation dispersion measurements have shed light on slower (microsecond/millisecond) motions, which may be more relevant in terms of function because catalytic turnover tends to happen on such a timescale (2,3). Information on alternative conformations has also come from NMR studies of proteins at high hydrostatic pressure, because high pressure increases the population of states that have a lower partial molar volume, which tend to be more ''open'' or unfolded states, related either to catalytic turnover or to unfolding (4–6). Pressure is also informative because of the following thermodynamic relationship:

$$\left\langle (\delta V)^2 \right\rangle = \kappa T V \beta_T, \qquad (1)$$

where $\langle(\delta V)^2\rangle$ is the average squared volume fluctuation, κ is the Boltzmann constant, T is the absolute temperature, V is the volume, and β_T is the isothermal compressibility coefficient (7). Equation 1 shows that compressibility is related to volume fluctuation, and means that measurements of compressibility (obtained, for example, by determining the structural change with pressure) also provide information on volume fluctuations at ambient pressure. Volume fluctuation is a useful parameter because it reports on protein flexibility. We previously determined the change in structure with pressure for the proteins lysozyme, bovine pancreatic trypsin inhibitor (BPTI), and staphylococcal protein G (8–10), and found that in all three proteins the largest compressibilities, and therefore the largest volume fluctuations, occur close to the active site (or, in the case of protein G, the site of binding to IgG). Moreover, in lysozyme and BPTI, the largest compressibility is also located close to buried water molecules, suggesting that buried water molecules are important for volume fluctuations (protein G does not contain buried water molecules). A number of studies have demonstrated that ligand binding tends to reduce the compressibility of proteins, implying that bound proteins have smaller fluctuations. Of interest, the compressibility of protein-ligand complexes seems to be related to their reactivity. For example, in dihydrofolate reductase (DHFR), large changes in compressibility occur with binding of different ligands; the most highly compressible state is the Michaelis complex (DHFR.NADPH.dihydrofolate), and the least compressible one is the product complex DHFR.NADP^{+}.tetrahydrofolate (11). We therefore performed a pressure-dependent NMR study of the well-characterized ribonuclease enzyme barnase, both free and in the presence of a deoxyribonucleotide inhibitor, d(CGAC).

Barnase is a small, stable enzyme and consists of a five-stranded β-sheet that forms a platform on top of which the ribonucleic acid substrate sits, surrounded by three helices and a number of loops and helical turns. Most of the interactions with substrate come from residues in the loops. Crystal structures of the free enzyme and of complexes with several nucleotide inhibitors, as well as its physiological partner

Submitted March 3, 2009, and accepted for publication June 15, 2009.

*Correspondence: m.williamson@sheffield.ac.uk

Editor: Josh Wand.

0006-3495/09/09/1482/9 $2.00

doi: 10.1016/j.bpj.2009.06.022

barstar, show that the structure changes very little on binding to substrate, but suggest that there is a loss of mobility in some regions, particularly in the active site (12,13). Barnase has been extensively studied by NMR, and resonance assignments (14) as well as ^{15}N relaxation parameters (15) are available. It shows substrate specificity for cleavage after guanine bases, and the binding site has a subsite where guanine binds, both in the crystal (13) and in solution (16). Therefore, barnase is a good system for studying changes in conformation and dynamics on ligand binding. Here, we present results from high-pressure NMR spectroscopy on free barnase and its complex with an inhibitor d(CGAC), which demonstrate major changes in compressibility and therefore in volume fluctuations on ligand binding. We suggest that the timescale for these fluctuations is in the relatively inaccessible intermediate range of nanoseconds to microseconds.

MATERIALS AND METHODS

Materials

^{13}C, ^{15}N-labeled barnase was purified as described previously (16). The ligand d(CGAC) was purchased from Metabion International AG (Martinsried, Germany) and used without further purification. Solid d(CGAC) was added to a solution of barnase to give an ~4.5-fold excess of ligand ([barnase] = 1.1 mM, [d(CGAC)] = 4.7 mM). Given the dissociation constant of 49 μM under our conditions (16), this provides >98% bound protein in the NMR tube.

NMR experiments

Experiments were carried out on a Bruker BioSpin (Karlsruhe, Germany) DRX-800 operating at 800 MHz for proton, as described previously (17). Chemical shift values at variable pressure were measured at 298 K using ^{15}N and ^{13}C HSQC spectra at 3 MPa (rather than at atmospheric pressure (0.1 MPa), to avoid the risk of getting small bubbles in the solution), and at 50, 100, 150, and 200 MPa. Data were processed using FELIX (Accelrys, San Diego, CA), and peaks were analyzed using Excel (Microsoft, Seattle, WA). Chemical shift assignments (14) were confirmed using standard triple resonance NMR experiments. For the ^{13}C HSQC spectra, folding was used in the indirect dimension, which means that there was some overlapping of side-chain signals. Consequently, the number of resolved and assigned shifts available for side-chain groups was limited. For free barnase, chemical shifts were followed for a total of 90 HN protons (all residues from 4 to 110, except for 21, 28, 38, 47, 51, 52, 57–59, 64, 67, 68, 78, 82, 84, 101, and 109, which were either overlapped or broadened) and 152 HC protons (59 CαH and 93 side-chain resonances), giving a total of 242 chemical shifts that could be used as restraints. For bound barnase, 89 HN, 49 CαH, and 84 other HC shifts were available. Several signals showed a nonlinear dependence of chemical shift on pressure. In earlier work (10), we showed that these nonlinear shifts are a consequence of an alternative structure that starts to become significantly populated at higher pressures. Here we were not interested in the alternative structure, so curved shifts were fitted to a parabolic function, and the linear part of the pressure dependence (in general equivalent to the shift on going from 3 to 100 MPa) was used to generate the structural restraint.

Structure calculation

The structure calculation method has been described previously (8–10,18). It is based on the premise that although ^{1}H chemical shifts alone cannot be calculated accurately enough for structure refinement, the change in chemical shift in response to a gradual change in structure can be used as a structural restraint, provided that the initial structure is known accurately and the structural change is small, as indeed it is here. We therefore start with a high-resolution crystal structure, and equilibrate it in the X-PLOR force field until it undergoes no further structural change. This equilibrated structure is defined as the starting structure. Chemical shifts are calculated for this starting structure using the PROTON routine in X-PLOR (19). Three sets of molecular dynamics (MD) trajectories are then calculated: one with no chemical shift restraints applied, to check that the structure is stable under the MD protocol; one that uses the calculated starting shifts, which by definition are the low-pressure shifts, and produces the low-pressure structure; and one that uses the calculated starting shifts to which are added the change in experimental shift between 3 and 200 MPa, which produces the high-pressure structure. Chemical shifts are converted to structural restraints within X-PLOR using previously derived simple geometrical relationships between structure and shift (20–22). The chemical shift restraints are applied with a strong force constant using a low temperature for the MD, implying that the chemical shifts are the dominant factor in the structure change. The calculation is therefore in effect a structural refinement based on chemical shift changes. Thus, the calculations produce valid structures even though they do not include solvent or ligand, since the dominant chemical shift terms both restrain and maintain the correct structure. The high-pressure structure is only of value when compared with the corresponding low-pressure structure; it is the difference in structure between these two calculations that defines how the structure changes on application of pressure. More complete details are provided in the Supporting Material.

The compressibility is calculated from the mean change in Cα coordinates with pressure. Cavity volumes were calculated with the use of MOLMOL (23), using a mean value for probe radii of 1.0, 1.1, 1.2, and 1.3 Å.

RESULTS

High-pressure structure of free barnase

NMR spectra were acquired for barnase at pressures between 3 and 200 MPa, and used to produce a set of ^{1}H chemical shift restraints that were then used to calculate structural changes between low and high pressure. Structures at low and high pressure were deposited in the Research Collaboratory of Structural Bioinformatics Protein Data Bank (PDB) (24) with codes 2kf3 (low) and 2kf4 (high), and shift restraints were deposited in BioMagResBank (25) with codes 16169 and 16170.

Three sets of structures were calculated and averaged to produce three resultant structures that describe how the structure of free barnase changes with pressure. The first is the ''no-shifts structure''. This structure is obtained without the use of chemical shift restraints, and the calculation is carried out as a check of the structural variability in the absence of chemical shift restraints. A ''low-pressure structure'' is obtained using as restraints the chemical shifts calculated for the initial structure. This structure is used a reference for the ''high-pressure structure'', which is calculated using the chemical shifts calculated as above, to which are added the change in experimental chemical shift values between low and high pressure. Table 1 demonstrates the clear structural change.

The structural change with pressure is <0.2 Å root mean-square (RMS), in line with our earlier results (8–10,18,26). The magnitude and nature of the structural changes are

TABLE 1 Mean RMS changes (Å) for backbone atoms between specified groups of structures or a group and a single other structure in free barnase

	Crystal	Initial*	No shifts*	Low *P**	High *P**
No shifts	1.16	0.24	0.23†	0.26	0.28
Low *P*	1.15	0.21	0.26	0.06†	0.16
High *P*	1.18	0.22	0.28	0.16	0.06†

*Initial structure was produced by iterated free dynamics refinement of the crystal structure, and used as the starting structure for the three subsequent calculations. The no-shifts calculation was unrestrained by chemical shifts, the low-*P* calculation used the shifts calculated from the initial structure as restraints, and the high-*P* structure used the sum of the calculated shifts plus the experimental difference between low- and high-pressure shifts.
†RMS difference between structures in the group.

very similar to those observed in crystal structures obtained at high pressure (27–31). Such small changes can be accurately probed using chemical shifts, which are sensitive to very small structural changes. The chemical shift restraints were well satisfied in the resultant structures: the mean absolute difference between target and resultant shift was 0.003 ppm, compared with a mean absolute change in shift of 0.046 ppm between 3 and 200 MPa. Previous studies used nuclear Overhauser effect (NOE) restraints to characterize the high-pressure structure of BPTI (31), where the NOE changes were fully consistent with the chemical shift-derived structural change (9), and to calculate the structure of ubiquitin (32), where structural changes of up to 3 Å were observed. However, in general, NOEs are not precise enough to provide useful restraints for structural changes as small as occurring here (33,34). Hydrogen-bond changes with pressure have also been analyzed using cross-hydrogen bond ^{3h}J couplings (35), yielding results consistent with the chemical shift-derived changes, so far as they can be interpreted in structural terms (10). These results, as well as cross-checks performed with different starting structures (reported in more detail in the Supporting Material and carried out previously on BPTI (9) and protein G (10)) validate the chemical shift method. A further powerful validation comes from the structural statistics shown in Tables 2 and 3, which demonstrate that the volumes decrease as expected. The structural changes are driven entirely by the chemical shift changes, which drive the reduction in volume without explicit ''high-pressure'' conditions. Nevertheless, the methodology used here is still relatively new and unconventional, and may therefore be subject to as yet unknown errors.

The change in structure with pressure is obtained by looking at the difference between the low- and high-pressure structures. These are compared in Fig. 1, from which it is clear that most of the changes occur in loops. However, the structural changes are small, and it is therefore important to check that the structural changes seen are not due merely to instabilities in the structure in that region. In other words, it is important to compare the difference against the no-shifts changes to make sure that we are not merely seeing random structural change. The result is shown in Fig. 2 *a*, in which the structural change is weighted by a ''reliability index'' obtained from the no-shifts calculations (Supporting Material). Here, red indicates a region of the structure undergoing a pressure-dependent change that is much larger than any possible structural variability, and blue indicates a change much smaller than that seen in the absence of restraints, and thus a region that is clearly identifiable as unchanging

TABLE 2 Structural statistics for free barnase at low and high pressure

	Low pressure	High pressure	High-low	High-low (%)
vdW volume (Å^3)*	12055(9)	12018(6)	−37	−0.3
Connolly volume (Å^3)*	21830(19)	21670(17)	−160	−0.7
Cavity volume (Å^3)†	119	121	−2	−12
Surface area (Å^2)‡	5802(13)	5743(15)	−59	−1.0
Radius of gyration (Å)§	13.41(0.006)	13.38(0.003)	−0.03	−0.2
Moment of inertia I_{xx} (Da Å^2)§	108002(159)	107384(148)	−618	−0.6
Moment of inertia I_{yy} (Da Å^2)§	59958(87)	59387(72)	−571	−1.0
Moment of inertia I_{zz} (Da Å^2)§	136508(159)	136483(89)	−25	−0.02

Calculated from an ensemble of 50 structures. Values in parentheses are the SDs. No SDs are given for the cavity volumes because these were calculated only from the averaged structures.
*Calculated using VOIDOO (70).
†Calculated using MOLMOL (23). Because the result is an average of different probe sizes, the mean percentage change in volume cannot be calculated directly from the previous columns. This also makes it difficult to estimate the error, although it could easily be 20% for the low- and high-pressure values and therefore much larger for the difference.
‡Calculated using CCP4 routine AREAMOL, part of the CCP4 suite (71).
§Calculated using X-PLOR from the average structure of the 50 structures. Very approximately, the *x* axis runs horizontally, the *y* runs vertically, and *z* comes out of the page in the orientations used here.

TABLE 3 Structural statistics for the barnase.d(CGAC) complex at low and high pressure

	Low pressure	High pressure	High-low	High-low (%)
vdW volume (Å^3)*	12024(11)	12019(11)	−5	−0.04
Connolly volume (Å^3)*	21516(28)	21519(25)	+3	+0.01
Cavity volume (Å^3)†	157	150	−7	−4.5
Surface area (Å^2)‡	5768(22)	5545(18)	−223	−3.9
Radius of gyration (Å)§	13.46(0.01)	13.45(0.01)	−0.01	−0.07
Moment of inertia I_{xx} (Da Å^2)§	68330(214)	68177(206)	−153	−0.22
Moment of inertia I_{yy} (Da Å^2)§	72692(195)	72871(183)	+179	+0.25
Moment of inertia I_{zz} (Da Å^2)§	165587(502)	165216(454)	−371	−0.22

Calculated from an ensemble of 50 structures. Values in parentheses are the SDs. No SDs are given for the cavity volumes because these were calculated only from the averaged structures.
*Calculated using VOIDOO (70). The small increase in Connolly volume is not significantly different from zero (Student's *t*-test).
†Calculated using MOLMOL (23).
‡Calculated using the CCP4 routine AREAMOL (71).
§Calculated using X-PLOR from the average structure of the 50 structures.

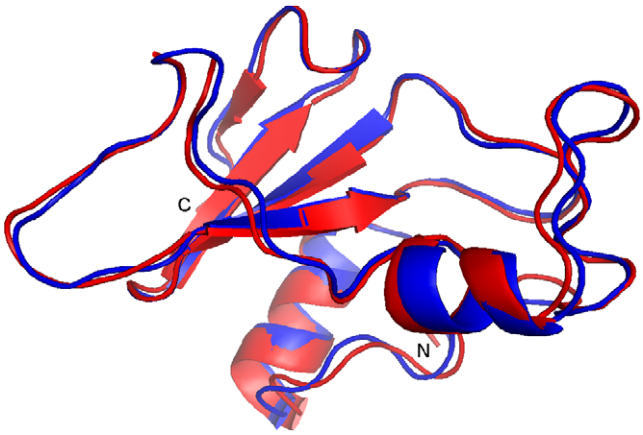

FIGURE 1 Comparison of structures of free barnase at low pressure (*blue*) and high pressure (*red*), superimposed using all backbone atoms. The differences from low to high have been multiplied by a factor of 5 to make it easier to see the changes. Structures were created using PyMOL (72).

with pressure. From this figure it is clear that the largest pressure-dependent changes are toward the front and top of the structure as shown, whereas the N-terminal helix at the back, together with the loops at the side, show the least change. The most variable residues (20–28, 48–50, and 54) form a cluster at the front of the structure together with 4 and 94–95. In particular, the 26–28 region is identified as strongly affected by pressure. We note that residue 27 is implicated in stabilizing the cleaved phosphate in the transition state (36). Changes in structure can also be analyzed by calculating the Voronoi volumes, i.e., the polyhedral volume of each atom in the structure. This is a ''noisy'' calculation, since atoms on the surface and next to cavities (which in our calculation did not contain buried water molecules) have undefined Voronoi surfaces. The results are therefore not shown, but are in agreement with those shown here.

Table 2 presents details of the changes in structure, demonstrating that the Connolly volume (i.e., the envelope volume of the protein) is compressed by ~0.7%, with the radius of gyration being reduced in proportion. This is an intrinsic isothermal compressibility of 3.7×10^{-11} Pa^{-1}, a figure that is comparable to values previously obtained by NMR and crystallography, which are mainly in the range of 0–5.3×10^{-11} Pa^{-1}, and within the range of partial specific abiabatic compressibilities measured for globular proteins using ultrasound (37). It is, however, small compared to the typical value of 25×10^{-11} Pa^{-1} calculated for the intrinsic compressibility from the partial specific compressibility by allowing for the effect of the solvent layer (38). This difference is discussed further in the Supporting Material. As expected, the van der Waals volume is much less compressible. Surface area is not a very useful parameter, as found in our earlier studies (8–10), because it is very sensitive to small changes in side-chain orientation. The most reliable indicator of structural change is the radius of gyration. The changes in the three orthogonal moments of inertia demonstrate that the compression is not uniform, although it is more uniform than seen in the three globular proteins we studied previously. Calculation of cavity volumes is very imprecise, but, as expected, the cavities (some of which contain buried water molecules) are found to be the most compressible parts of the protein.

Hydrogen-bond lengths are compressed (by 0.027 ± 0.075 Å, or ~1%), and there is a wide variation in changes in the hydrogen bonds, with many increasing in length. Overall, however, they are relatively compressible in comparison with the structure as a whole. Therefore, by far the most compressible parts of the protein are the cavities, followed by noncovalent interactions (such as hydrogen bonds), and finally the covalent structure, which is almost incompressible.

High-pressure structure of barnase bound to d(CGAC)

Similar calculations were carried out for barnase bound to the deoxynucleotide inhibitor d(CGAC), and data were deposited in the PDB with codes 2k5f (low) and 2kf6 (high), and in BioMagResBank with codes 16171 and 16172. As for free barnase, the chemical shift restraints were well satisfied (mean absolute change in shift: 0.063 ppm for HN and 0.036 ppm for HC; mean absolute error in structures: 0.004 ppm). Pressure-induced changes in structure are given in Table 3. By comparison with the results for free barnase shown in Table 2, the overall structural change is much smaller. The Connolly volume is essentially unchanged and the radius of gyration decreases by only 0.07%, implying that the complex is much less compressible (by ~70%) than free barnase. The changes in the moments of inertia are quite different from those in free barnase, demonstrating that the nature of the structural change is different. Hydrogen bonds compress by a mean value of 0.027 Å (the same as in free barnase, within error), but again with a large standard deviation (SD). There appears to be considerably less compressibility in the cavities than in free barnase.

These conclusions are confirmed by analyzing the locations of structural change, which are shown in Fig. 2 *b*. The residues that were affected by pressure in free barnase are now almost invariant, with the most variable residues remaining close to the N- and C-termini. This is shown more clearly by calculating the difference in structural changes between free and bound barnase (Fig. 2 *c*), which shows that there is a major ''freezing'' of the structure at the front of the protein, particularly around residues 26–28 and 54, with a smaller increase in structural change in the bound state for the N- and C-termini. The figure also demonstrates that the freezing of the structure extends to a number of other residues in the β-sheet, and many of the residues that contact the ligand clearly have much reduced variability in the bound state. Of interest, many of these residues also make contacts with buried water molecules (Fig. 2 *c*).

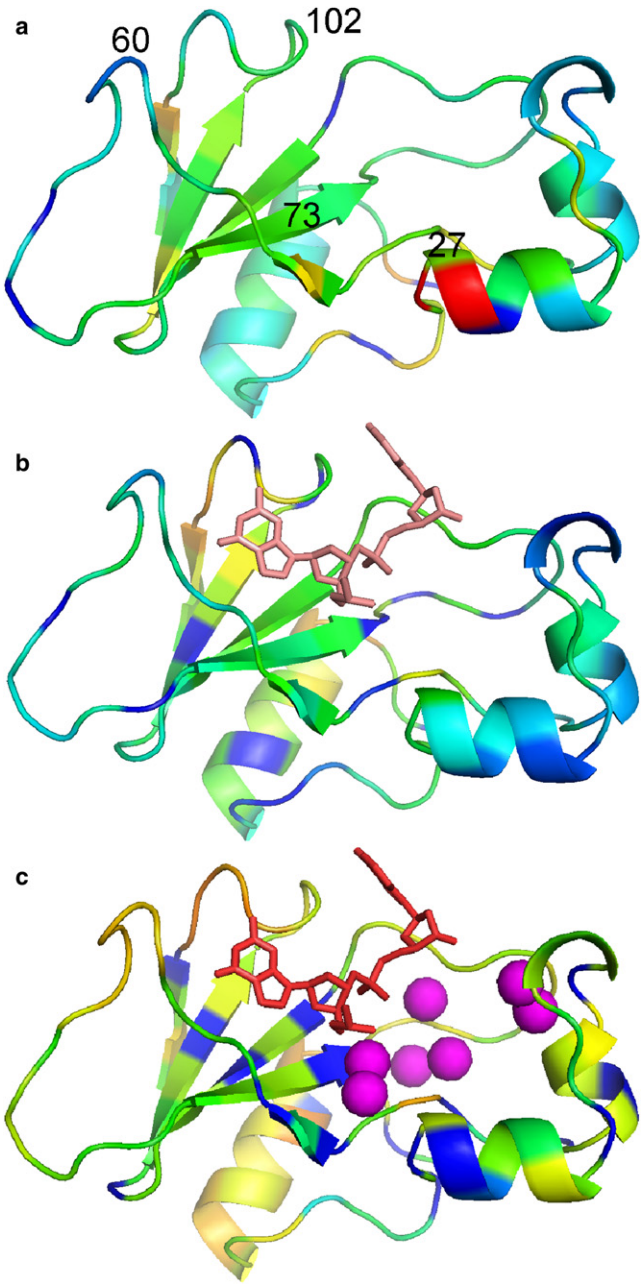

FIGURE 2 Change in structure of barnase between low and high pressure. (*a*) Differences in Cα coordinates for free barnase, minus the mean variation in Cα coordinates in the ''no-shifts'' structures. Red indicates a region of the structure undergoing a pressure-dependent change that is much larger than any possible structural variability, through orange and yellow to green, indicating a change similar to that seen in the absence of restraints, and finally to blue, indicating a change much smaller than that seen in the absence of restraints, and thus a region that is clearly identifiable as unchanging with pressure. Blue, cyan, green, orange, and red correspond to differences of ~ -0.2, -0.1, 0, 0.1, and $\geq$ 0.2 Å, respectively. For orientation, some key residues are indicated. Lys-27 hydrogen bonds to the cleaved phosphate and is thought to form key interactions in the transition state; the loop from 57 to 60 is the guanine recognition loop, which forms interactions with G^2; and the active site general base and acid residues are Glu-73 and His-102. (*b*) Same difference for bound barnase; same color scheme. The location of the ligand (nucleotides G^2 and A^3 of bound d(CGAC)) is indicated. The crystal structure 1brn does not have electron density for nucleotide 1, whereas cytosine 4 makes no contacts with the protein and has significantly higher crystallographic *B* factors; nucleotides 2 and 3 therefore represent the entire bound ligand. (*c*) Difference in Cα movement, bound minus free (i.e., the difference between *a* and *b*). Residues that alter less in bound barnase compared to free are in blue, and residues that alter more are in red; orange, yellow, green, and blue correspond to $\sim$0.15, 0, -0.1, and ≤ -0.2 Å, respectively. Also shown are nucleotides 2 and 3 of the ligand, together with the solvent-inaccessible water molecules (*purple spheres*). The residues colored blue are 23, 26, 28, 34, 40, 44, 50, 53, 55, 75, 87, 89, 93, 97, and 107.

DISCUSSION

In this study we measured the changes in protein structure with pressure for free and bound barnase. These structural changes reflect differences in compressibility. Therefore, we present for the first time (to our knowledge) an experimental study that shows in atomic detail changes in protein compressibility resulting from binding to a ligand. Our results only give the structural change of the protein component, and provide no information on the solvent layer. This layer is ~1 molecule thick and has a compressibility ~75% of that of bulk water (18,39), which varies according to the nature of the protein surface (40). Although the compressibility of the solvent layer affects compressibilities measured using ultrasound or thermodynamic measurements, it has no effect on the measurements reported here.

The results of several thermodynamic studies of compressibility changes (11,41–45) provide an average compressibility and in general show that compressibility is reduced on binding, either to small molecules or to other proteins. Compressibility changes have ranged from 1% to 73%. The overall change in compressibility seen here is large: a reduction of ~70%. Of interest, Kamiyama and Gekko (11) measured changes in compressibility for dihydrofolate reductase bound to a range of ligands, which ranged from a decrease in compressibility compared to free enzyme of 19% up to an increase of 15%. The most compressible structure was the Michaelis complex, DHFR.NADPH.tetrahydrofolate, whereas the least compressible was the reaction product, DHFR.$NADP^+$.dihydrofolate. In other words, the greatest compressibility was seen for the ''most active'' complex, and the least compressibility was observed for the ''least active''. We also note that in studies of lysozyme complexes, the change in compressibility was observed to increase with size and potency of oligo-*N*-acetyl glucosamine inhibitor as GlcNAc 17%, $GlcNAc_2$ 27%, and $GlcNAc_3$ 73% (42). Thus, one can tentatively conclude that the least active/most inhibited enzyme structures are also the least compressible. Our results are consistent with this general idea, since there is a large reduction in compressibility in the inhibited complex. There is an interesting parallel with amyloidosis, where the toxic species, the protofibrils, are highly compressible (46) but the mature fibrils are not (47).

On binding to d(CGAC), there is a dramatic reduction in structural change for residues close to the ligand binding site (and in particular close to the active site), and a smaller

increase in structural change for residues far from the ligand-binding site. The result is consistent with our earlier studies, which showed the greatest structural changes in lysozyme, BPTI, and protein G close to the active site. We have also noted for lysozyme and BPTI that the largest changes in structure are close to buried water molecules. Our results on barnase are consistent with this (Fig. 2 *c*), and support the view that buried waters contribute greatly to the conformational flexibility of proteins (48).

What is the significance of the compressibility measurements? Many years ago, the relationship indicated by Eq. 1, which shows that compressibility is proportional to mean-square volume fluctuation, was noted. This is a thermodynamic relationship that applies to the whole system and not necessarily to individual components of it. However, it does apply to local regions at high frequencies (small volume changes), where structural change is very localized (49). Moreover, experimental results obtained by NMR (8–10), crystallography (50), and optical methods (51) suggest that it applies reasonably well across a wide range of fluctuations, although fluctuations in the protein are clearly correlated or ''slaved'' to fluctuations in the solvent (52,53).

The results reported here therefore demonstrate that in free barnase, volume fluctuations are greatest close to the ligand-binding site, and also close to the buried water molecules. When barnase is bound to inhibitor, the volume fluctuations close to the ligand-binding site are almost completely quenched, although fluctuations elsewhere in the structure become slightly greater. From Eq. 1, the RMS volume fluctuations for free and bound barnase are respectively ~60 and 30 $Å^3$, representing a functionally relevant magnitude, if concentrated in a limited region of the protein, as was the case here. It is worth pointing out that, because chemical shift changes are linear with pressure and therefore compressibilities are constant with pressure, the volume fluctuations are essentially independent of pressure; that is, although our results were obtained by varying the pressure, our conclusions on volume fluctuations also hold true at ambient pressure.

This result demonstrates that the parts of the enzyme that are required to contact the substrate are those that are subject to the greatest fluctuations. In essence, this is what the induced fit mechanism suggests. However, it is even more consistent with the conformational selection or preequilibrium/population shift hypothesis (54–56), which states that the free enzyme is in equilibrium between a low-energy inactive state and a family of higher-energy active states, at least one of which is capable of binding to the ligand and moving on rapidly to the transition state, and that binding of the ligand to the higher-energy state selects this state and shifts the equilibrium. Specifically, it requires that the free enzyme be already in a dynamic equilibrium. Recent NMR studies using relaxation dispersion measurements have shown that several enzymes are indeed in an equilibrium between two states, with the higher-energy state resembling the next stage in the catalytic cycle (56). It is important to note that the results shown here reveal a different (though most likely related) phenomenon: in the ground state, the enzyme displays conformational fluctuations precisely in those regions that will be required to accommodate the ligand (Fig. 3).

Barnase has been studied by MD simulations, in the free state, and in complex with its inhibitor barstar (57,58) and substrates GpA and GpAp (59). Motions were shown to comprise residues 24–5, 50–55, 71–75, and 87–91, which were suggested to form a hinge between two rigid domains that changes its dynamics in response to ligand binding. The MD simulations suggested that this is a concerted slow motion. This hinge motion is suggested to be a good model for the motions necessary for conformational selection in barnase. There is good correspondence between these hinge residues and the residues observed here to undergo volume fluctuations (see Fig. 2 legend), implying that the two observations are closely related, though not identical.

Enzymes undergo conformational fluctuations on a large number of timescales. ^{15}N relaxation studies of barnase revealed small-scale motions of the backbone, uniformly distributed over the whole protein (except for increased mobility at the termini), occurring on a subnanosecond timescale (15). Such motions are observed for all proteins, and are caused by thermal motion; effectively, the protein moves because the constant bombardment by water molecules

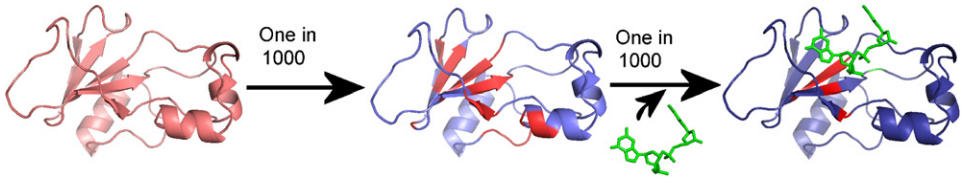

FIGURE 3 Diagrammatic hypothetical mobility of barnase. The enzyme undergoes small-scale rapid (picosecond–nanosecond) motions (colored *pink*) that occur with essentially equal magnitude all over the protein. These motions occasionally (very roughly once in 1000 vibrations, i.e., on a nanosecond–microsecond timescale) occur in a concerted manner to give larger scale and less frequent fluctuations (shown in *red*); these are the motions characterized here. Even more rarely (again roughly once in 1000 occurrences and thus on a microsecond–millisecond timescale) these fluctuations come together to generate a highly localized motion that has been observed by relaxation dispersion in several enzymes, including barnase (M. J. Pandya, C. J. Craven and M. P. Williamson, unpublished observations), to produce a fluctuation that could be described as hinge bending, and is set up to bind productively to the substrate and go on to react. There is thus a channeling of many small, uncorrelated motions into a small number of concerted motions. The red residues in the central image correspond approximately to those found to have high compressibility in free barnase but not in bound barnase (i.e., the *blue* residues in Fig. 2 *c*, smoothed and omitting the residues in the 34–40 loop since these show high variability in calculations). The red residues in the right-hand panel correspond approximately to the central hinge-bending region characterized by MD (58,59). The figure is not intended to imply at what point the ligand binds.

forces it to move. Observations of side-chain dynamics in barnase showed a similar pattern (58). By contrast, catalytic turnover in barnase occurs on a timescale of milliseconds (60), and accumulating evidence suggests that this timescale is in general dictated not by the rate of the chemical reactions themselves, which are much faster, but by the rate of conformational change of the enzyme as it responds to the changing structure of its ligand. The kinetic energy for the conformational change must come from motions already occurring within the enzyme. It was suggested many years ago that larger-scale motions, involving concerted movement in many different parts of the protein, are statistically unlikely, which is why they occur far less frequently than the small-scale rapid motions (61,62); essentially, there is a channeling of small-scale rapid motions into rarer concerted motions (Fig. 3). For example, the flipping of an aromatic ring in the protein interior requires a concerted motion of the surrounding side chains, with an activation volume of ~40 $Å^3$, and generally occurs on a submicrosecond timescale, or more slowly in tightly packed regions (63,64). The volume fluctuations observed here are clearly slower than picosecond/nanosecond, since there is no correlation between results from ^{15}N relaxation studies (15) and compressibilities (R^2 for free barnase compressibility versus $S^2 = 0.00$; compressibility change free to bound versus change in S^2 free to barstar bound = 0.04). On the other hand, they are faster than microsecond/millisecond, since 1), we observe no exchange broadening of these resonances, specifically of residues 26–28, which show the greatest compressibility in the free state; and 2), relaxation dispersion measurements of the free protein show no obvious effects around 26–28, although effects are observable in other parts of the protein, specifically in regions identified as close to the hinge in MD simulations, namely, 56 and 83–86 (M. J. Pandya, C. J. Craven and M. P. Williamson, unpublished observations). We previously reached similar conclusions for the volume fluctuations in BPTI (65). We conclude that the fluctuations observed here are intermediate in their timescale (i.e., the nanosecond–microsecond timescale). This would fit with the scale of the correlated motion, which is intermediate in magnitude between random uncorrelated rapid motions and the highly correlated motions required for the transitions to the activated state (Fig. 3). The magnitude of the volume fluctuation observed here (60 $Å^3$) is consistent with this timescale, and thus the data demonstrate that fluctuations of intermediate magnitude occur on an intermediate timescale. It is therefore suggested that the fluctuations characterized here form an intermediate stage in the funneling of rapid uncorrelated dynamics into the correlated motions required for function. We note that pressure perturbation is a novel way to identify such fluctuations, which to date have only been accessible by analyzing the averaging of residual dipolar couplings (66–68).

The fluctuations seen for the free enzyme are almost entirely quenched in the d(CGAC) complex. As noted above, this observation is in agreement with compressibility measurements on lysozyme and dihydrofolate reductase (11,42). However, it does not agree with relaxation dispersion measurements on dihydrofolate reductase, which detect conformational exchange for all complexes in the catalytic cycle (69). The explanation for this discrepancy probably lies in the fact that the compressibility measurements report on motions in the nanosecond/microsecond timescale, whereas relaxation dispersion measurements report on the microsecond/millisecond timescale. Therefore, by combining these experiments, it may be possible to characterize the complete ''dynamic channel'', which narrows and changes as the timescale lengthens and the magnitude of the fluctuation increases (Fig. 3).

SUPPORTING MATERIAL

Additional text, references, and figures are available at http://www.biophysj.org/biophysj/supplemental/S0006-3495(09)01155-2.

We thank K. Hata (Kinki University, Kinokawa, Japan) for carrying out the cavity volume calculations.

Funding for this study was provided by the Biotechnology and Biological Sciences Research Council (grants BB/D015308/1 and BB/D521230/1).

REFERENCES

1. Goodey, N. M., and S. J. Benkovic. 2008. Allosteric regulation and catalysis emerge via a common route. *Nat. Chem. Biol.* 4:474–482.
2. Hansen, D. F., P. Vallurupalli, and L. E. Kay. 2008. Using relaxation dispersion NMR spectroscopy to determine structures of excited, invisible protein states. *J. Biomol. NMR.* 41:113–120.
3. Loria, J. P., R. B. Berlow, and E. D. Watt. 2008. Characterization of enzyme motions by solution NMR relaxation dispersion. *Acc. Chem. Res.* 41:214–221.
4. Akasaka, K. 2003. Highly fluctuating protein structures revealed by variable-pressure nuclear magnetic resonance. *Biochemistry.* 42: 10875–10885.
5. Akasaka, K. 2006. Probing conformational fluctuation of proteins by pressure perturbation. *Chem. Rev.* 106:1814–1835.
6. Jonas, J. 2002. High-resolution nuclear magnetic resonance studies of proteins. *Biochim. Biophys. Acta.* 1595:145–159.
7. Cooper, A. 1976. Thermodynamic fluctuations in protein molecules. *Proc. Natl. Acad. Sci. USA.* 73:2740–2741.
8. Refaee, M., T. Tezuka, K. Akasaka, and M. P. Williamson. 2003. Pressure-dependent changes in the solution structure of hen egg-white lysozyme. *J. Mol. Biol.* 327:857–865.
9. Williamson, M. P., K. Akasaka, and M. Refaee. 2003. The solution structure of bovine pancreatic trypsin inhibitor at high pressure. *Protein Sci.* 12:1971–1979.
10. Wilton, D. J., R. B. Tunnicliffe, Y. O. Kamatari, K. Akasaka, and M. P. Williamson. 2008. Pressure-induced changes in the solution structure of the GB1 domain of protein G. *Proteins.* 71:1432–1440.
11. Kamiyama, T., and K. Gekko. 2000. Effect of ligand binding on the flexibility of dihydrofolate reductase as revealed by compressibility. *Biochim. Biophys. Acta.* 1478:257–266.
12. Meiering, E. M., M. Bycroft, M. J. Lubienski, and A. R. Fersht. 1993. Structure and dynamics of barnase complexed with 3′-GMP studied by NMR spectroscopy. *Biochemistry.* 32:10975–10987.
13. Buckle, A. M., and A. R. Fersht. 1994. Subsite binding in an RNAse: structure of a barnase tetranucleotide complex at 1.76 Å resolution. *Biochemistry.* 33:1644–1653.

14. Korzhnev, D. M., E. V. Bocharov, A. V. Zhuravlyova, E. V. Tischenko, M. Y. Reibarkh, et al. 2001. ^{1}H, ^{13}C and ^{15}N resonance assignment for barnase. *Appl. Magn. Reson.* 21:195–201.
15. Sahu, S. C., A. K. Bhuyan, J. B. Udgaonkar, and R. V. Hosur. 2000. Backbone dynamics of free barnase and its complex with barstar determined by ^{15}N NMR relaxation study. *J. Biomol. NMR.* 18:107–118.
16. Cioffi, M., C. A. Hunter, M. Pandya, M. J. Packer, and M. P. Williamson. 2009. Use of quantitative ^{1}H NMR chemical shift changes for ligand docking into barnase. *J. Biomol. NMR.* 43:11–19.
17. Kamatari, Y. O., R. Kitahara, H. Yamada, S. Yokoyama, and K. Akasaka. 2004. High-pressure NMR spectroscopy for characterizing folding intermediates and denatured states of proteins. *Methods.* 34:133–143.
18. Wilton, D. J., M. Ghosh, K. V. A. Chary, K. Akasaka, and M. P. Williamson. 2008. Structural change in a B-DNA helix with hydrostatic pressure. *Nucleic Acids Res.* 36:4032–4037.
19. Kuszewski, J., A. M. Gronenborn, and G. M. Clore. 1995. The impact of direct refinement against proton chemical shifts on protein structure determination by NMR. *J. Magn. Reson. B.* 107:293–297.
20. Williamson, M. P., and T. Asakura. 1993. Empirical comparisons of models for chemical shift calculation in proteins. *J. Magn. Reson. B.* 101:63–71.
21. Williamson, M. P., J. Kikuchi, and T. Asakura. 1995. Application of ^{1}H NMR chemical shifts to measure the quality of protein structures. *J. Mol. Biol.* 247:541–546.
22. Asakura, T., K. Taoka, M. Demura, and M. P. Williamson. 1995. The relationship between amide proton chemical shifts and secondary structure in proteins. *J. Biomol. NMR.* 6:227–236.
23. Koradi, R., M. Billeter, and K. Wüthrich. 1996. MOLMOL: a program for display and analysis of macromolecular structures. *J. Mol. Graph.* 14:51–55.
24. Berman, H. M., J. Westbrook, Z. Feng, G. Gilliland, T. N. Bhat, et al. 2000. The Protein Data Bank. *Nucleic Acids Res.* 28:235–242.
25. Ulrich, E. L., H. Akutsu, J. F. Doreleijers, Y. Harano, Y. E. Ioannidis, et al. 2008. BioMagResBank. *Nucleic Acids Res.* 36:D402–D408.
26. Iwadate, M., T. Asakura, P. V. Dubovskii, H. Yamada, K. Akasaka, et al. 2001. Pressure-dependent changes in the structure of the melittin α-helix determined by NMR. *J. Biomol. NMR.* 19:115–124.
27. Kundrot, C. E., and F. M. Richards. 1987. Crystal structure of hen egg-white lysozyme at a hydrostatic pressure of 1000 atmospheres. *J. Mol. Biol.* 193:157–170.
28. Urayama, P., G. N. Phillips, and S. M. Gruner. 2002. Probing substates in sperm whale myoglobin using high-pressure crystallography. *Structure.* 10:51–60.
29. Collins, M. D., M. L. Quillin, G. Hummer, B. W. Matthews, and S. M. Gruner. 2007. Structural rigidity of a large cavity-containing protein revealed by high-pressure crystallography. *J. Mol. Biol.* 367:752–763.
30. Colloc'h, N., E. Girard, A.-C. Dhaussy, R. Kahn, I. Ascone, et al. 2006. High pressure macromolecular crystallography: the 140-MPa crystal structure at 2.3 Å resolution of urate oxidase, a 135-kDa tetrameric assembly. *Biochim. Biophys. Acta.* 1764:391–397.
31. Li, H., H. Yamada, and K. Akasaka. 1999. Effect of pressure on the tertiary structure and dynamics of folded basic pancreatic trypsin inhibitor. *Biophys. J.* 77:2801–2812.
32. Kitahara, R., S. Yokoyama, and K. Akasaka. 2005. NMR snapshots of a fluctuating protein structure: ubiquitin at 30 bar-3 kbar. *J. Mol. Biol.* 347:277–285.
33. Neuhaus, D., and M. P. Williamson. 2000. The Nuclear Overhauser Effect in Structural and Conformational Analysis. Wiley-VCH, New York.
34. Williamson, M. P. 2009. Applications of the NOE in Molecular Biology. *In* Annual Reports on NMR Spectroscopy. G. A. Webb, editor. Academic Press, New York. 77–109.
35. Li, H., H. Yamada, K. Akasaka, and A. M. Gronenborn. 2000. Pressure alters electronic orbital overlap in hydrogen bonds. *J. Biomol. NMR.* 18:207–216.
36. Mossakowska, D. E., K. Nyberg, and A. R. Fersht. 1989. Kinetic characterization of the recombinant ribonuclease from *Bacillus amyloliquefaciens* (barnase) and investigation of key residues in catalysis by site-directed mutagenesis. *Biochemistry.* 28:3843–3850.
37. Gekko, K., and Y. Hasegawa. 1986. Compressibility-structure relationship of globular proteins. *Biochemistry.* 25:6563–6571.
38. Chalikian, T. V. 2003. Volumetric properties of proteins. *Annu. Rev. Biophys. Biomol. Struct.* 32:207–235.
39. Marchi, M. 2003. Compressibility of cavities and biological water from Voronoi volumes in hydrated proteins. *J. Phys. Chem. B.* 107:6598–6602.
40. Dadarlat, V. M., and C. B. Post. 2006. Decomposition of protein experimental compressibility into intrinsic and hydration shell contributions. *Biophys. J.* 91:4544–4554.
41. Filfil, R., A. Ratavosi, and T. V. Chalikian. 2004. Binding of bovine pancreatic trypsin inhibitor to trypsinogen: spectroscopic and volumetric studies. *Biochemistry.* 43:1315–1322.
42. Gekko, K., and K. Yamagami. 1998. Compressibility and volume changes of lysozyme due to inhibitor binding. *Chem. Lett. (Jpn.).* 27:839–840.
43. Filfil, R., and T. V. Chalikian. 2003. Volumetric and spectroscopic characterizations of glucose-hexokinase association. *FEBS Lett.* 554:351–356.
44. Filfil, R., and T. V. Chalikian. 2003. The thermodynamics of protein-protein recognition as characterized by a combination of volumetric and calorimetric techniques: the binding of turkey ovomucoid third domain to α-chymotrypsin. *J. Mol. Biol.* 326:1271–1288.
45. Barbosa, S., P. Taboada, D. Attwood, and V. Mosquera. 2003. Thermodynamic properties of the complex formed by interaction of two anionic amphiphilic penicillins with human serum albumin. *Langmuir.* 19:10200–10204.
46. Akasaka, K., A. R. A. Latif, A. Nakamura, K. Matsuo, H. Tachibana, et al. 2007. Amyloid protofibril is highly voluminous and compressible. *Biochemistry.* 46:10444–10450.
47. Meersman, F., and C. M. Dobson. 2006. Probing the pressure-temperature stability of amyloid fibrils provides new insights into their molecular properties. *Biochim. Biophys. Acta.* 1764:452–460.
48. Fischer, S., and C. S. Verma. 1999. Binding of buried structural water increases the flexibility of proteins. *Proc. Natl. Acad. Sci. USA.* 96: 9613–9615.
49. Yu, X., and D. M. Leitner. 2003. Vibrational energy transfer and heat conduction in a protein. *J. Phys. Chem. B.* 107:1698–1707.
50. Tilton, R. F., J. C. Dewan, and G. A. Petsko. 1992. Effects of temperature on protein structure and dynamics: x-ray crystallographic studies of the protein ribonuclease-A at 9 different temperatures from 98 K to 320 K. *Biochemistry.* 31:2469–2481.
51. Scharnagl, C., M. Reif, and J. Friedrich. 2005. Local compressibilities of proteins: comparison of optical experiments and simulations for horse heart cytochrome *c*. *Biophys. J.* 89:64–75.
52. Pfeiffer, H., K. Heremans, and M. Wevers. 2008. The influence of correlated protein-water volume fluctuations on the apparent compressibility of proteins determined by ultrasonic velocimetry. *Biochim. Biophys. Acta.* 1784:1546–1551.
53. Fenimore, P. W., H. Frauenfelder, B. H. McMahon, and R. D. Young. 2004. Bulk-solvent and hydration-shell fluctuations, similar to α- and β-fluctuations in glasses, control protein motions and functions. *Proc. Natl. Acad. Sci. USA.* 101:14408–14413.
54. Bosshard, H. R. 2001. Molecular recognition by induced fit: how fit is the concept? *News Physiol. Sci.* 16:171–173.
55. Tsai, C. J., B. Y. Ma, and R. Nussinov. 1999. Folding and binding cascades: shifts in energy landscapes. *Proc. Natl. Acad. Sci. USA.* 96:9970–9972.
56. Boehr, D. D., H. J. Dyson, and P. E. Wright. 2006. An NMR perspective on enzyme dynamics. *Chem. Rev.* 106:3055–3079.
57. Nolde, S. B., A. S. Arseniev, V. Y. Orekhov, and M. Billeter. 2002. Essential domain motions in barnase revealed by MD simulations. *Proteins.* 46:250–258.
58. Zhuravleva, A., D. M. Korzhnev, S. B. Nolde, L. E. Kay, A. S. Arseniev, et al. 2007. Propagation of dynamic changes in barnase upon

binding of barstar: an NMR and computational study. *J. Mol. Biol.* 367:1079–1092.

59. Giraldo, J., L. De Maria, and S. J. Wodak. 2004. Shift in nucleotide conformational equilibrium contributes to increased rate of catalysis of GpAp versus GpA in barnase. *Proteins.* 56:261–276.
60. Day, A. G., D. Parsonage, S. Ebel, T. Brown, and A. R. Fersht. 1992. Barnase has subsites that give rise to large rate enhancements. *Biochemistry.* 31:6390–6395.
61. Henzler-Wildman, K., and D. Kern. 2007. Dynamic personalities of proteins. *Nature.* 450:964–972.
62. Lumry, R., and H. Eyring. 1954. Conformation changes of proteins. *J. Phys. Chem.* 58:110–120.
63. Wagner, G. 1980. Activation volumes for the rotational motion of interior aromatic rings in globular proteins determined by high-resolution ^{1}H NMR at variable pressure. *FEBS Lett.* 112:280–284.
64. Hattori, M., H. Li, H. Yamada, K. Akasaka, W. Hengstenberg, et al. 2004. Infrequent cavity-forming fluctuations in HPr from *Staphylococcus carnosus* revealed by pressure- and temperature-dependent tyrosine ring flips. *Protein Sci.* 13:3104–3114.
65. Akasaka, K., H. Li, H. Yamada, R. H. Li, T. Thoresen, et al. 1999. Pressure response of protein backbone structure. Pressure-induced amide ^{15}N chemical shifts in BPTI. *Protein Sci.* 8:1946–1953.
66. Lange, O. F., N. A. Lakomek, C. Farès, G. F. Schröder, K. F. A. Walter, et al. 2008. Recognition dynamics up to microseconds revealed from an RDC-derived ubiquitin ensemble in solution. *Science.* 320:1471–1475.
67. Bouvignies, G., P. Bernado, S. Meier, K. Cho, S. Grzesiek, et al. 2005. Identification of slow correlated motions in proteins using residual dipolar and hydrogen-bond scalar couplings. *Proc. Natl. Acad. Sci. USA.* 102:13885–13890.
68. Tolman, J. R., J. M. Flanagan, M. A. Kennedy, and J. H. Prestegard. 1997. NMR evidence for slow collective motions in cyanometmyoglobin. *Nat. Struct. Biol.* 4:292–297.
69. Boehr, D. D., D. McElheny, H. J. Dyson, and P. E. Wright. 2006. The dynamic energy landscape of dihydrofolate reductase catalysis. *Science.* 313:1638–1642.
70. Kleywegt, G. J., and T. A. Jones. 1994. Detection, delineation, measurement and display of cavities in macromolecular structures. *Acta Crystallogr. D Biol. Crystallogr.* 50:178–185.
71. Bailey, S. 1994. The CCP4 suite: programs for protein crystallography. *Acta Crystallogr. D Biol. Crystallogr.* 50:760–763.
72. DeLano, W. L. 2002. The PyMOL Molecular Graphics System. DeLano Scientific, Palo Alto, CA.